Process Safety and Environmental Protection 148 (2021) 846–857

Contents lists available at ScienceDirect

Process Safety and Environmental Protection

journal homepage: www.elsevier.com/locate/psep

Feasibility of electrochemical regeneration of activated carbon used in drinking water treatment plant. Reactor configuration design at a pilot scale

Borja Ferrández-Gómez [a], Diego Cazorla-Amorós [b], Emilia Morallón [a,*]

[a] Materials Institute of Alicante and Department of Physical Chemistry, University of Alicante, 03080 Alicante, Spain
[b] Materials Institute of Alicante and Department of Inorganic Chemistry, University of Alicante, 03080 Alicante, Spain

ARTICLE INFO

Article history:
Received 22 December 2020
Received in revised form 27 January 2021
Accepted 3 February 2021

Keywords:
Electrochemical regeneration
Activated carbon
Anode
Reactor configuration
Adsorption
Bisphenol A

ABSTRACT

This work evaluates the feasibility of electrochemical regeneration of granular activated carbon used in drinking water treatment plants as a real alternative to thermal regeneration. Two pilot-plant-scale reactors, with a capacity of 10−15 kg, have been designed using two different configurations, parallel plate electrodes and concentric cylindrical electrodes. The optimization of the anode material has also been studied and Pt/Ti, RuO_2/Ti and IrO_2/Ti have been used. After the regeneration and, thus, recovery of the porosity the samples were tested in the adsorption of bisphenol A. In the electrochemical regeneration, recovery of the porosity of spent activated carbon until 100 % and 96 % with respect to the pristine activated carbon using Pt/Ti anode after 3 h of treatment, has been achieved. The regeneration process produces a small increase in the number of surface oxygen groups. No important differences have been observed among the tested anodes and RuO_2/Ti and IrO_2/Ti can be an economic alternative to Pt/Ti. Bisphenol A adsorption kinetics was slower in regenerated activated carbons probably due to the formation of surface oxygen groups. However, the adsorption capacity was similar in the regenerated samples and the pristine one.

1. Introduction

The growing demand for water reuse, which is increasingly inaccessible to the population, together with the development of advanced water treatment processes and the adoption of more restrictive environmental protection legislation, has caused that the global production of activated carbon (AC) increases annually by about 10 % (Zanella et al., 2014). This is because adsorption on AC is an advanced technology established to remove organic and inorganic pollutants present in water (Radovic et al., 2001; Shabir et al., 2020) and it is considered as a universal adsorbent of common use in water treatment plants.

However, the management of spent AC, when the adsorption capacity is partial or fully depleted, is difficult since it may be considered as a highly pollutant waste. Consequently, the viability of the use of AC at the industrial level, and with increasing amounts, will depend on their efficient regeneration and the appropriate management necessary to ensure the sustainability of the adsorption process.

The conventional process of industrial AC regeneration is thermal regeneration in an inert atmosphere or under oxidative conditions. It is a method that achieves high efficiency (85–90 %) of AC regeneration but has some disadvantages (Muñoz et al., 2007; Berenguer et al., 2010a) such as high energy consumption (EC), modification of textural properties due to undesirable effects of gasification of the carbon material, between 10–20 % of material is lost, release of pollutant gases and high transportation costs since it is a process that is applied *off-site* (Salvador et al., 2015a). In addition, the number of companies that can regenerate AC is limited.

To reduce these problems, several alternative methods of regeneration of AC have been developed including chemical, microbiological and vacuum technologies (Salvador et al., 2015b). The electrochemical process stands out as one of the most interesting alternatives to the thermal method for its high efficiency, lower cost, low EC, low CO_2 emissions, can be applied to other adsorbent materials, and it is an environmentally friendly technology (Berenguer et al., 2010b).

* Corresponding author.
E-mail address: morallon@ua.es (E. Morallón).

https://doi.org/10.1016/j.psep.2021.02.007

Advances in recovery of adsorption capacity from spent AC through electrochemical methods have mainly focused on laboratory-scale studies that use low amount of ACs. These studies provide a regeneration efficiency higher than 85 % depending on the experimental variables (McQuillan et al., 2018). These electrochemical regeneration processes have been carried out using the common types of reactor design (Walsh and Ponce de León, 2018), including: a) parallel plate electrodes in a rectangular flow channel, b) concentric cylindrical electrodes, c) rotating cylinder electrodes, d) bipolar trickle towers containing 3-D electrode layers and e) fluidized bed electrodes, with divided and undivided compartments.

Among the laboratory-scale reactors developed for electrochemical regeneration of adsorbent materials, we should highlight those designed with a column configuration with cylindrical electrodes (Narbaitz and McEwen, 2012; Zanella et al., 2017) and those designed and constructed as a reactor with parallel plate electrodes (Narbaitz and Karimi-Jashni, 2012; Sharif et al., 2017).

Regardless of regeneration type, cathodic or anodic, the regeneration mechanism involves oxidation processes by electrogenerated active species such as active chlorine, ozone, hydrogen peroxide (H_2O_2) and hydroxyl radicals, *via* indirect anodic oxidation, or by electrogenerated H_2O_2 through indirect cathodic oxidation, together with electrostatic repulsion as consequence of the polarization of the AC due to the electric field (Zhan et al., 2016). The formation of H_2O_2 is relatively easy to occur as the reduction of oxygen can take place at a wide range of pH values and is favoured on steel and carbon electrodes (Berenguer et al., 2009; McQuillan et al., 2018). Therefore, the efficiency of electrochemical regeneration is influenced by the nature of the electrode material. According to Pletcher and Walsh (1993) and Martínez-Huitle et al. (2015), the electrode must have: a) high physicochemical stability, b) being resistant to corrosion and formation of passive layers, c) enough electrical conductivity, d) high catalytic activity and e) low cost and high durability. For these reasons, in laboratory-scale reactors and with non-commercial anodes, different materials such as graphite (Weng and Hsu, 2008), boron-doped diamond (Acuña-Bedoya et al., 2020), Pt (Narbaitz and McEwen, 2012), Ti (Huang et al., 2017), Pt/Ti (Ding et al., 2020; Liu et al., 2020) and stainless steel (Karabacakoğlu and Savlak, 2014) have been used obtaining a regeneration efficiency between 60–90 %. To reduce economic costs and reach optimal regeneration efficiencies, dimensionally stable anodes (DSA) such as RuO_2/Ti (Dai et al., 2017), RuO_2/IrO_2/Ti (Zhan et al., 2018), SnO_2/Ti (Wang and Balasubramanian, 2009) and, IrO_2/Ti (Brown et al., 2004) have been used since these electrodes have shown excellent electrocatalytic properties, electromechanical properties and resistance to corrosion and can influence the voltage of the electrochemical cell. In addition, low EC and high current efficiency are obtained using DSA electrodes (Krstić and Pešovski, 2019).

Regarding the prototypes developed at bench-scale, two electrochemical reactors with parallel plate electrodes configuration were built and used to regenerate saturated AC in laboratory conditions with phenol and 4,4′-diamino stilbene-2,2′-disulfonic acid (Wang and Balasubramanian, 2009) and saturated in real conditions in a drinking water treatment plant (DWTP) (Ferrández-Gómez et al., 2021).

DWTP companies are nowadays facing with an important problem with the use of AC due to the stricter legislation, what results in an increasing production of spent AC. Considering that spent AC is an important problem nowadays in this industry, this work shows the feasibility for the application of the electrochemical method for the regeneration of spent AC from DWTP. From the scaling-up process that it was previously developed (Ferrández-Gómez et al., 2021), we have designed and built a pilot-plant-scale prototype to treat 15 kg of AC per batch with parallel plate electrode configuration and concentric cylindrical electrode configuration. For both prototypes proposed, the anode composition has been optimized and the pristine and regenerated ACs have been tested in the adsorption of an emerging pollutant such as bisphenol A (BPA) due to its widespread presence in the environment and its endocrine disruption properties (Xiao et al., 2020) and because it has been also studied in a significant piece of literature, what is of interest for data interpretation.

2. Materials and methods

2.1. Materials and chemicals

The granular AC used was AquaSorb®F23 (10 × 40 mesh, Jacobi Carbons, France) and this material was used during 3 years in El Realón municipal DWTP in Spain. The AC was used in the plant for the removal of a large number of compounds that affect the odour and taste of water, in unknown concentration, and inorganic matter, also in unknown concentration, from the raw water provided by rivers and wells for improving the organoleptic properties of water.

Sulfuric acid (analytical grade, VWR International, USA) water solution was used as electrolyte and it was prepared with tap water for the electrochemical regeneration experiments. BPA (2,2-Bis(4-hydroxyphenyl) propane) (synthesis grade, Merck kGaA, Germany) was used as pollutant; the BPA solution was prepared in ultrapure water (18.2 MΩ cm, Elga-Vivendi, UK) for the adsorption in solution tests.

Three commercial mesh anodes: Ti mesh fully platinized, Ti mesh coated with Ru mixed metal oxide (MMO), and Ti mesh coated with Ir MMO (Magneto, The Netherlands) were purchased and machined to adapt them to the two different reactor configurations. In addition, these commercial anodes were characterized by different techniques and named as Pt/Ti, RuO_2/Ti and IrO_2/Ti, respectively. In addition, in both prototypes developed in this work, 304-stainless steel (SS) was used as cathode material as an economical alternative to Pt/Ti (Ferrández-Gómez et al., 2021).

In order to test the effect of the contact of the AC with the electrolyte, a washing treatment of 6 g of spent AC was done by keeping it in agitation for 1 h by magnetic stirrer with 200 mL of an electrolytic aqueous solution of 0.5 M H_2SO_4.

2.2. Electrochemical regeneration of activated carbon

2.2.1. Parallel plate electrode reactor

This reactor (Fig. 1A) was designed and built with parallel plate electrodes configuration (labelled as PPR). It was built in polyvinyl chloride (PVC) in two compartments of 72 cm × 57 cm × 10 cm separated by a cationic membrane (Ionac MC-3470, LANXESS Sybron Chemicals Inc., USA) with an effective area of 1800 cm^2. Each compartment was connected to one polystyrene tank. The electrolyte outlet was connected horizontally in the lower part of the tank. The tank serves as electrolyte reservoir. The electrolyte is kept under continuous flow using two magnetic pumps (P0253, Plastomec, Italy). The anodes were placed in close contact with the cationic membrane so that the electrode-to-electrode distance was fixed to 10.5 cm. A current density of 250 A/m^2 was set for all experiments and it was supplied by a power source (GE050250DVR, Grelco, Spain) operating in galvanostatic mode.

For each experiment, 15 kg of spent AC were placed into the cathodic compartment and treated using 0.5 M of H_2SO_4 as electrolyte, 75 L in each tank, with a flow rate of 750 L/h for 4 h. Given that the compartment volume was 35,000 cm^3, the residence time in PPR was 168 s. The different experiments performed were named PPR1, PPR2 and PPR3 for Pt/Ti, RuO_2/Ti and IrO_2/Ti anode, respec-

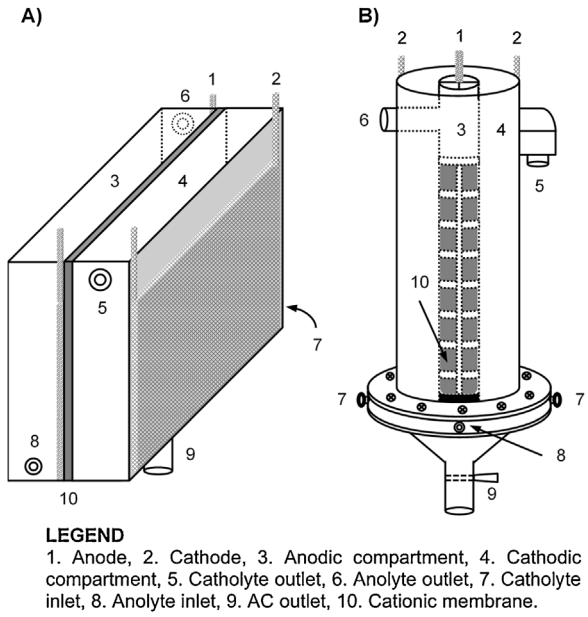

Fig. 1. Schemes of the two electrochemical prototypes constructed at pilot-plant-scale: A) Parallel plate reactor and B) Concentric cylindrical reactor.

tively, and SS as cathode with a geometric area of the electrodes of 2800 cm^2.

2.2.2. Concentric cylindrical electrode reactor

The second reactor (Fig. 1B) was designed and built with concentric cylindrical electrodes configuration (labelled as CCR). The reactor was built also in PVC and constructed in two cylindrical concentric compartments, external and internal, with a diameter of 30 and 10 cm, respectively, and 130 cm of height that are electrochemically connected through the cationic membrane, which total area is 1050 cm^2. The anode was placed in close contact with the cationic membrane so that the anode-to-cathode distance was fixed to 10.5 cm, and the same current density than in the case of PPR was used. Each compartment was connected to one tank, with the electrolyte outlet horizontally connected in the lower part of the tank, through PVC pipes and two magnetic pumps kept the electrolyte continuously flowing from the reactor compartment to the electrolyte reservoir.

For each experiment, 10 kg of spent AC were placed into the cathodic compartment and regenerated at 27.5 A using 0.5 M of H_2SO_4 as electrolyte, 70 L in the cathodic and 30 L in the anodic tanks, with a flow rate of 750 L/h for 4 h. Given that the compartment volume was 31,414 cm^3, the residence time in CCR was 153 s. The experiments were named as CCR1, CCR2 and CCR3 for Pt/Ti, RuO_2/Ti and IrO_2/Ti anodes, respectively, located in the internal compartment, and SS as cathode. Both electrodes with a geometric area of 1080 cm^2.

2.3. Characterization of activated carbon

Sampling was carried out at different points of the AC bed and mixed to obtain a homogenized sample of regenerated AC. Each sample obtained was washed with abundant distilled water until neutral pH and dried at 70 °C for overnight.

The porous texture of pristine, spent, and regenerated AC samples was determined by N_2 adsorption-desorption isotherms at -196 °C and CO_2 adsorption isotherms at 0 °C using an automatic adsorption system (Autosorb-6B, Quantachrome Corporation, USA). 100 mg of AC were outgassed at 150 °C under vacuum for 8 h. Total volume of micropores ($V_{DR}(N_2)$) and volume of narrow micropores ($V_{DR}(CO_2)$) were calculated applying the Dubinin-Radushkevich (DR) equation (Dubinin, 1960), the volume of mesopores (V_{meso}) was calculated by subtraction of the adsorbed volume at relative pressures of 0.9 and 0.2 and the apparent specific surface area was determined by the Brunauer-Emmet-Teller (BET) equation (Lozano-Castelló et al., 2009). The pore size distribution (PSD) was calculated by applying the bidimensional non-local density functional theory method (2D-NLDFT) to the N_2 adsorption isotherms using SAIEUS software (version 2.0, Micromeritics Instrument Corp. 2000–2015) (Jagiello and Olivier, 2012). The percentage of recovery of porosity (%RP) was calculated as the ratio of BET surface area (S_{BET}) of regenerated to pristine AC according to the Eq. (1). However, to get a more detailed assessment of the recovery of porosity, the percentage of adsorption recovery (%AR) was also calculated using the Eq. (2). This equation takes into account the initial state of the spent AC prior to the regeneration.

$$\%RP = \frac{S_{BET,\ regenerated\ AC}}{S_{BET,\ pristine\ AC}} \cdot 100 \quad (1)$$

$$\%AR = \frac{S_{BET,\ regenerated\ AC} - S_{BET,\ spent\ AC}}{S_{BET,\ pristine\ AC} - S_{BET,\ spent\ AC}} \cdot 100 \quad (2)$$

The surface chemistry of ACs was analysed by temperature-programmed desorption (TPD) experiments. These were performed in a DSC-TGA equipment (Simultaneous TGA/DSC SDT Q600, TA Instruments, USA) coupled to a mass spectrometer (HiCube 80 Eco, Pfeiffer Vacuum, Germany) which was used to follow the *m/z* lines related to the decomposition of surface functional groups from the AC. The thermobalance was purged for 45 min under He flow rate of 100 mL/min and then heated up to 950 °C (heating rate 20 °C/min). In addition, the pH at the point of zero charge (pH_{PZC}) was determined using the procedure previously described by Such-Basáñez et al. (2004). This analysis consists of contacting a certain amount of AC with ultrapure water in continuous stirring in a thermostatic bath at 25 °C for 24 h. The amounts of AC used were (0.05, 0.1, 0.5, 1, 5 and 10 wt%), the solid was filtered and the pH of the solution was measured.

The surface morphology of ACs were studied by scanning electron microscope (SEM) (S-3000 N, Hitachi, Japan), which was coupled to a Rontec X-ray detector for energy dispersive X-ray (EDX) analysis.

2.4. Characterization of commercial anodes

The surface morphology and composition of the different anodes was studied by SEM which was coupled to a Rontec X-ray detector for EDX analysis. The microstructure and crystallinity were characterized by X-ray diffraction (XRD) in a diffractometer (Bruker D8-Advance, Billerica, USA) by using a CuK_α ($\lambda = 0.1541$ nm) radiation source at a step of 0.05°/s in the 2θ range from 10° to 80°. X-ray photoelectron spectroscopy (XPS) measurements were carried out by an spectrometer (VG-Microtech Multilab 3000, Thermo Electron Corporation, UK) with MgK_α radiation (1256.3 eV). Binding energies were referenced against the main C(1 s) line of adventitious carbon impurities at 284.6 eV.

The electrochemical behaviour of the commercial electrodes was studied by cyclic voltammetry (CV) using a potentiostat (VMP3, BioLogic, France) in a conventional three-electrode cell. The counter electrode was a Pt wire and the reference electrode were immersed in the electrolyte solution. The aqueous 1 M H_2SO_4 electrolyte solution was prepared in ultrapure water and was deoxygenated by N_2 bubbling. The cyclic voltammograms were obtained at a constant scan rate of 50 mV/s and the potential range was 0.1–1.4 V (*vs* Ag/AgCl). The roughness factor was calculated using the geometric area of the electrodes, 2 cm^2.

2.5. Bisphenol A adsorption tests and modelling

For the BPA adsorption tests, 300 mg of AC were put in contact with 200 mL of BPA solution (250 mg/L) into Erlenmeyer flasks, without buffer solution, which were then covered and kept in a water thermostatic bath at 25 °C and under agitation for 6 days. Samples were periodically taken to determine the amount of BPA adsorbed as a function of time. The amount adsorbed was determined by UV–vis spectroscopy at 277 nm using a spectrophotometer (V-670 UV–vis-NIR, Jasco, Japan). The adsorption capacity of BPA at different times, q (mg/g), was calculated according to the mass balance of Eq. (3):

$$q\,(mg/g) = \frac{(C_0 - C)}{m} \cdot V \quad (3)$$

where C_0 and C are initial and different time concentrations of BPA (mg/L), respectively, V (L) is the volume of the BPA solution and m (g) is the weight of AC.

The kinetic of the adsorption process can be controlled by the adsorption step or by diffusion. In this work, pseudo-first-order model, pseudo-second-order model and Elovich kinetic models, that describe the adsorption on surface sites, and the intraparticle diffusion model, assuming that film diffusion is negligible, were applied to the experimental data to analyse the adsorption mechanism.

The pseudo-first-order model, also named as the Lagergren equation (Lagergren, 1898), permits a simple kinetic evaluation of the adsorption of an adsorbate between two phases and can be represented by the Eqs. (4), (5):

$$\frac{dq}{dt} = k_1(q_e - q) \quad (4)$$

$$\ln(q_e - q) = \ln q_e - k_1 t \quad (5)$$

where q_e (mg/g) is the amount of BPA adsorbed per mass of AC at equilibrium conditions and q (mg/g) is the amount adsorbed at time t (h) and k_1 is the Lagergren rate constant of adsorption (h^{-1}).

In the pseudo-second-order kinetic model (Ho and McKay, 1999), the driving force (q_e-q) is proportional to the available fraction of active sites and can be represented by Eqs. (6), (7):

$$\frac{dq}{dt} = k_2(q_e - q)^2 \quad (6)$$

$$\frac{t}{q} = \frac{1}{k_2 q^2{}_e} + \frac{t}{q^2{}_e} \quad (7)$$

where k_2 is the pseudo-second-order rate constant of adsorption (g/mg/h).

The Elovich kinetic model (Kamgaing et al., 2017) has general application to chemisorption kinetics and is valid for systems in which the adsorbent surface is heterogeneous and can be represented by the Eqs. (8), (9):

$$\frac{dq}{dt} = \beta \exp(\alpha\beta) \quad (8)$$

$$q = \frac{1}{\beta}\ln(\alpha\beta) + \frac{1}{\beta}\ln t \quad (9)$$

where β (g/h) and α (mg/g/h) are the adsorption rate and the desorption constant.

Intraparticle diffusion model assumes that the film diffusion is negligible (Weber and Morris, 1963) and can be represented by the Eqs. (10), (11):

$$q = f\left(t^{1/2}\right) \quad (10)$$

$$q = k_{int} t^{1/2} \quad (11)$$

where k_{int} is intraparticle diffusion rate constant ($mg/g/h^{0.5}$).

2.6. Energy consumption of electrochemical regeneration

The EC per unit mass of regenerated AC was calculated according to the Eq. (12):

$$EC\,(kWh/kg) = \frac{U \cdot I \cdot t}{w \cdot 1000} \quad (12)$$

where U is the average voltage of the electrochemical cell (V), I is the applied current (A), t is the regeneration time (h) and w is the mass of AC (kg).

3. Results and discussion

3.1. Parallel plate reactor configuration

Fig. 2 presents the N_2 adsorption-desorption isotherms of the pristine, spent and after washing AC, and electrochemical regenerated ACs using the different anodes in the PPR configuration. Table 1 summarizes the main textural properties, such as the S_{BET}, $V_{DR}(N_2)$, $V_{DR}(CO_2)$ and V_{meso} for all these materials. All the isotherms are of type I (Thommes et al., 2015) corresponding to essentially microporous ACs; the small slope for relative pressures above 0.2 and the small hysteresis cycle, shows that the mesopores contribution is not important, in agreement with data in Table 1. PSD determined by application of 2D-NLDFT method to the N_2 adsorption-desorption isotherms are also plotted in Fig. 2.

The results for the pristine AC and the spent AC, show a clear decrease in porosity after the use of the AC for 3 years. It must be noted that although the porosity available in the spent AC is still important, its porous texture has the values that makes the DWTP companies to decide its replacement. After the electrochemical regeneration process, in all cases, a recovery of the adsorption capacity was observed compared to the spent one. It must be noted that, after 1 h of regeneration treatment, a recovery of porosity above 90 % is achieved for the three anodes tested. Interestingly, for Pt/Ti anode (samples PPR1), after 3 h of regeneration, a recovery of porosity of 100 % is reached (there is a very good overlapping between the N_2 adsorption-desorption isotherms of the pristine and regenerated sample, Fig. 2A). This is not obtained for the other two anodes in which higher regeneration times are detrimental in the recovery of porosity. The PSD for the pristine and regenerated AC have a well-defined microporosity distribution centred at 0.7 nm (Fig. 2A) and are similar in all cases, showing that the electrochemical regeneration does not produce a significant change in porosity, such as a widening of the micropores to meso and macropores as observed in previous studies (Moore et al., 2003; Narbaitz and McEwen, 2012; Ferrández-Gómez et al., 2021).

If we focus on the effect of the regeneration time, we find that in all cases an increase in time does not produce an increase in the recovery of porous properties, but it reaches a maximum and then decreases. This is in agreement with the observations by other authors where longer times does not result in a significant improvement in the recovery of porosity, but it can produce a larger EC (Liu et al., 2017; McQuillan et al., 2018; Santos et al., 2020).

In most of the cases, a full recovery of the textural properties is not achieved due to electrochemical oxidation or reduction of compounds desorbed from the spent AC, that can be adsorbed, and also to the AC oxidation itself (Berenguer et al., 2009; Wang and Balasubramanian, 2009; Ferrández-Gómez et al., 2021). This last aspect is discussed below. The above processes may be favoured with an increase in the current, applied voltage and regeneration time, thus producing increased blockage of the porosity (Ania and Béguin, 2008; Wang and Balasubramanian, 2009). For this reason, the regeneration efficiency may decrease if severe experimental conditions are used (Karabacakoğlu and Savlak, 2014; Salvador et al., 2015b). However, the interesting results with Pt/Ti anode

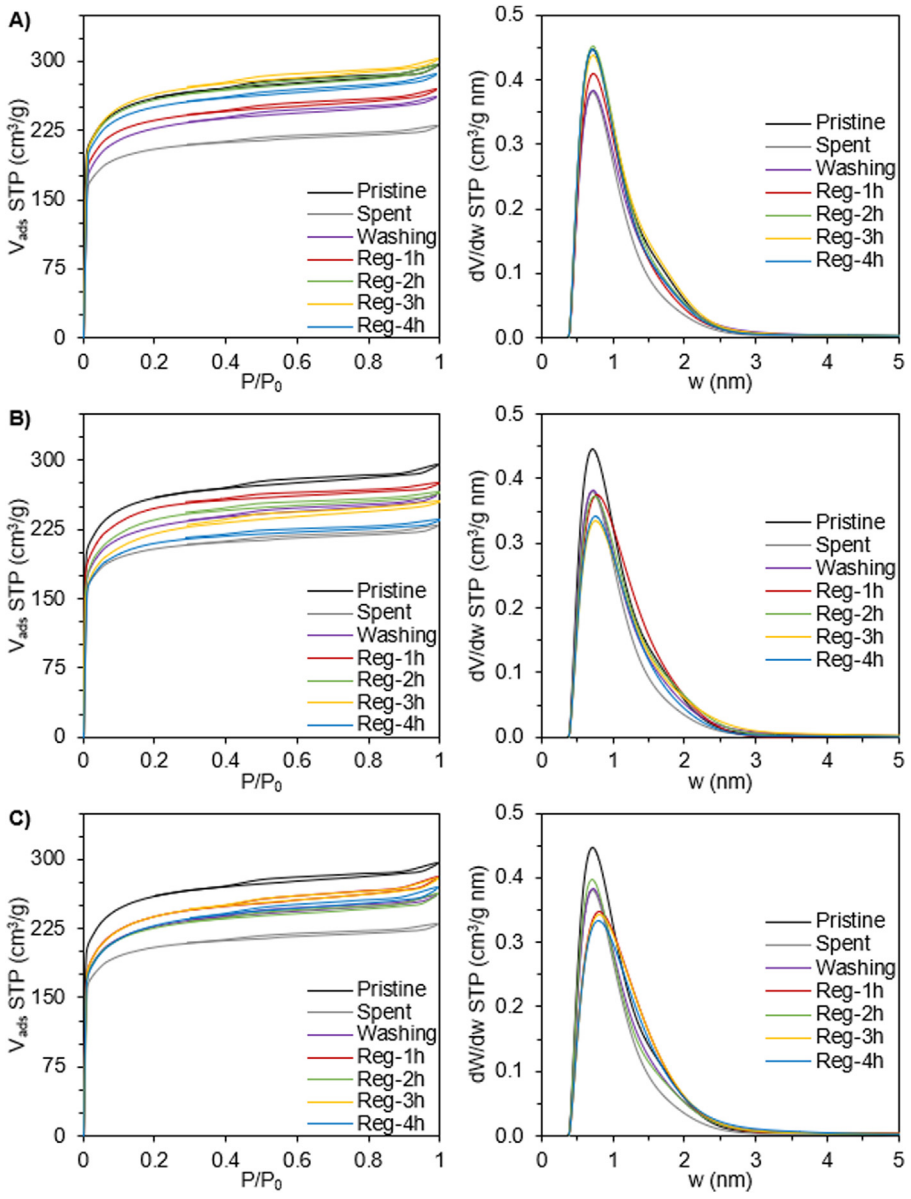

Fig. 2. N_2 adsorption-desorption isotherms at −196 °C and PSD for samples obtained from the experiments carried out in electrochemical regeneration of spent AC in a PPR configuration prototype: A) PPR1 (Pt/Ti), B) PPR2 (RuO_2/Ti) and C) PPR3 (IrO_2/Ti). The data for pristine, spent and washing AC are also included for comparison purposes.

must be emphasized since complete recovery of porosity at the experimental conditions used is reached.

Surface chemistry of the pristine, spent, and regenerated ACs was characterized by TPD experiments and by measurement of pH_{PZC}. Fig. 3**A** shows the TPD profiles for CO and CO_2 evolutions for the pristine, spent and electrochemically regenerated ACs for the Pt/Ti experiment carried out with the PPR configuration reactor (see Fig. S**2** in Supporting Information for TPD profiles for RuO_2/Ti and IrO_2/Ti in the PPR configuration). TPD for the spent AC after washing with acid electrolyte is also included. Table 1 summarizes the quantification of the CO and CO_2 evolved in these TPD experiments. This table also includes the pH_{PZC} and the total oxygen content calculated as CO + 2CO_2. Surface oxygen groups on carbon materials decompose during heating producing CO and CO_2 at different temperatures and the decomposition temperature is associated with specific types of oxygen groups. The evolution of CO occurs by decomposition of anhydrides (400–600 °C) and basic or neutral groups such as, phenols (600–700 °C) and carbonyl or quinones (700–900 °C). CO_2 evolves at lower temperatures as consequence of decomposition of acid groups like carboxylic acids (200–500 °C), anhydrides (400–600 °C) and lactones (600–800 °C) (Figueiredo et al., 1999).

Pristine AC has a low amount of surface oxygen groups and a basic pH_{PZC}, values which are typical of AC. The spent AC has a much higher CO and CO_2 desorption and a lower pH_{PZC}. This reveals that the AC is oxidized during the use in the DWTP (the AC bed is located after the oxidation step and some oxidizing species can reach the AC). Some of the CO and CO_2 evolution can be due to the decomposition of inorganic compounds like carbonates. This is reasonable considering that the analysis of the spent AC by EDX (Table S**4**) shows the presence of Ca in a significant amount (2.45 wt%). The water treated in this DWTP is hard water what explains the increase in the inorganic matter content with the time of use. The TPD profile for the spent AC after washing with the acidic electrolyte (Fig. 3) shows a decrease in CO and CO_2 evolution due to the removal of the inorganic compounds with the acidic treatment (in agreement with the decrease in elements as Ca measured by EDX). In any case,

Table 1
Physicochemical characterization of textural properties by N_2 and CO_2 adsorption-desorption isotherms, TPD and pH_{PZC} of pristine, spent, washing and electrochemical regenerated AC in parallel plate reactor configuration. All experiments were carried out with 15 kg of spent AC, under cathodic conditions, applying 70 A during 4 h, using 0.5 M H_2SO_4 as electrolyte solution and a flow rate of 750 L/h.

Sample	S_{BET} m^2/g	V_{DR,N_2} cm^3/g	V_{DR,CO_2} cm^3/g	V_{meso} cm^3/g	%RP	%AR	CO μmol/g	CO_2 μmol/g	O μmol/g	pH_{PZC}
Pristine	995	0.36	0.30	0.04			566	178	922	10.4
Spent	790	0.32	0.24	0.03			2668	1462	5592	7.3
Washing	870	0.35	0.25	0.04	87	30	2275	1361	4997	2.1
PPR1 (Pt/Ti)										
Reg-1h	910	0.34	0.27	0.04	92	59	2928	867	4663	2.2
Reg-2h	955	0.40	0.32	0.04	96	81	3095	791	4677	1.9
Reg-3 h	1020	0.41	0.27	0.04	103	112	3294	820	4935	1.9
Reg-4h	970	0.39	0.25	0.04	98	88	3202	907	5015	1.8
PPR2 (RuO_2/Ti)										
Reg-1h	945	0.37	0.30	0.03	95	76	2892	839	4570	2.2
Reg-2h	900	0.36	0.29	0.03	91	54	2520	750	4020	1.9
Reg-3 h	840	0.34	0.27	0.04	84	24	2889	1055	4998	1.9
Reg-4h	800	0.33	0.27	0.03	80	5	2960	874	4708	2.0
PPR3 (IrO_2/Ti)										
Reg-1h	910	0.37	0.28	0.04	92	59	3422	947	5315	2.1
Reg-2h	870	0.35	0.28	0.04	87	39	3725	989	5703	2.1
Reg-3 h	910	0.37	0.28	0.04	92	59	3292	917	5127	1.9
Reg-4h	875	0.35	0.27	0.04	88	42	3149	866	4882	2.0

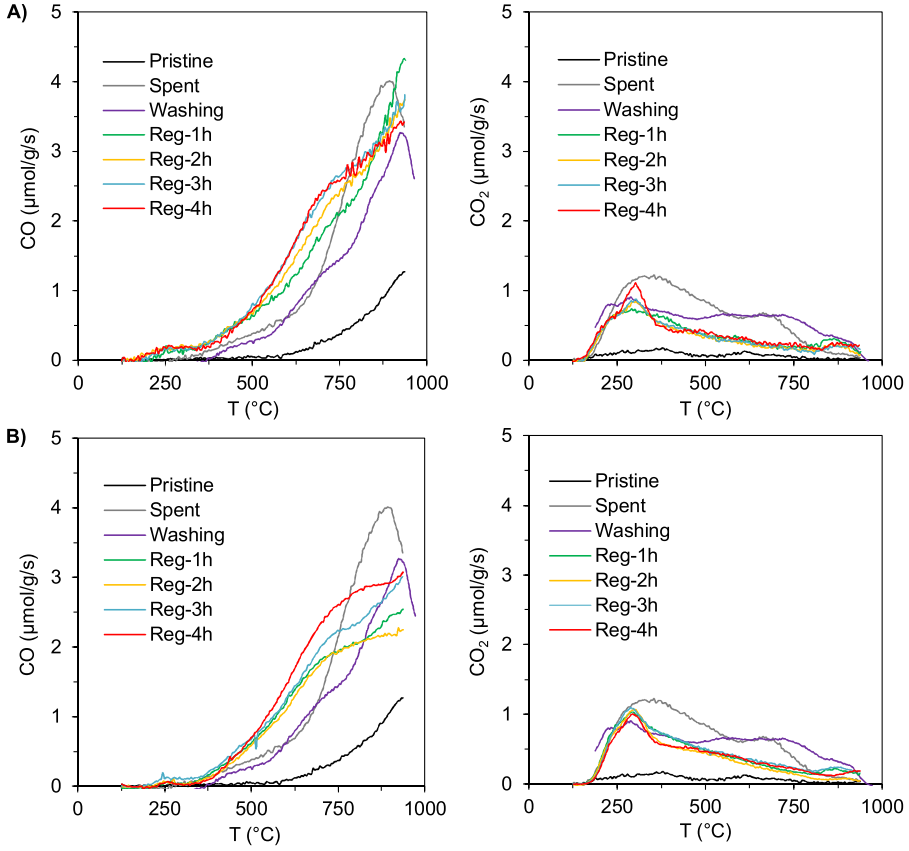

Fig. 3. CO and CO_2 TPD evolution profiles of the ACs regenerated for the electrochemical regeneration using a Pt/Ti anode in: A) PPR configuration and, B) CCR configuration. The data for pristine, spent and washing ACs are also included for comparison purposes.

the TPD of the spent AC after washing confirms that oxidation of the AC occurs during its use in the DWTP.

The surface chemistry of the electrochemically regenerated ACs can be compared with the pristine and spent AC after washing because all of them are free of the inorganic species that produce additional features in the TPD. After the regeneration treatment the CO evolution increases with respect to the pristine and the spent AC after washing with acidic electrolyte, showing that the regeneration treatment produces some additional oxidation of the AC generating phenol and carbonyl type CO groups (see the increase in CO desorption in the region of temperature between 500 and 800 °C, Figs. 3, **S2**–**S3**), although this additional oxidation depends on the anode used. However, the CO_2 profile shows a decrease in the high temperature region compared to the AC after washing, indicating that longer contact time with the electrolyte favours further removal of inorganic species. The pH_{PZC} reaches values around 2 in all the cases, due to the formation of acidic groups like carboxylic acids (Rivera-Utrilla et al., 2011), what is in agreement with the

observed CO_2 desorption at temperatures around 280 °C, which is much higher than for the pristine AC (Figs. 3, **S2**-**S3**). This decrease in pH is also observed in the spent AC after washing with the electrolyte, in agreement with the oxidation of the AC during its use.

Although the electrochemical regeneration has been performed under cathodic conditions, the oxidation of the carbon surface observed agrees with previous results (Berenguer et al., 2009; Gineys et al., 2017). It can be explained considering the oxidizing character of H_2O_2 species formed during the electrochemical oxygen reduction in the cathode, because the electrolyte is not deoxygenated (Delpeux-Ouldriane et al., 2015).

3.2. Optimization of anode composition in a parallel plate reactor

The characterization by SEM, XPS and XRD of three commercial electrodes proposed as anodes for the electrochemical regeneration of AC (**Figs. S4–S13** and Tables S**1–S3**) provides information about the chemical composition and crystallinity of the materials, as well as morphology. As can be seen, only platinum was detected by XPS and XRD in the Pt/Ti anode. However, for RuO_2/Ti and IrO_2/Ti the coatings also contain Ti, indicating that the anodes are composed by a mixture of RuO_2 or IrO_2 with TiO_2. The amount of Ru and Ir are 2 and 18.5 at%, respectively.

Fig. S**4** shows the voltammograms obtained for the different anodes in H_2SO_4. It can be observed that the voltammograms for MMO anodes show pseudo-capacitance behaviour. The oxidation state of Ru and Ir changes during the potential scan. This solid-state surface redox transition coupled with proton transfer gives rise to pseudo-capacitance behaviour and featured curves with current peaks. Voltammetric charge recorded in a potential range where gas is not evolved can be used to estimate the electrochemically active surface area and the roughness factor. The roughness factor (R_f) has been estimated from the experimental capacitances and the theoretical ones being 80 μF/cm^2 for RuO_2/Ti and IrO_2/Ti electrodes (Grupioni et al., 2002). In the case of Pt/Ti electrode it has been determined from the redox processes associated to the reduction of surface platinum oxide (Ureta-Zañartu et al., 1996) that corresponds to 224 μC/cm^2. The R_f obtained for each electrode was 18, 223 and 507, respectively. Also, as can be seen in Fig. S**4**, the IrO_2 anode is the most electroactive anode for the oxygen evolution reaction (OER).

The optimization of the anode composition on the regeneration efficiency can be explained considering that cathodic regeneration mechanism occurs through the electric field generated that contributes to the desorption of the adsorbed molecules and to the electro-generation in the cathode of peroxide species. Alternatively, H_2O_2 also can be further reduced at the cathode to form hydroxyl radicals and superoxide species or transformed in the presence of an AC surface within a three-phase system, shown by Eqs. (13)–(17) (Martínez-Huitle et al., 2015; Salvador et al., 2015b; McQuillan et al., 2018), responsible for the oxidation of the AC surface and adsorbed organic compounds. The oxygen molecules formed in the anode and the lack of deoxygenation are responsible for the formation of the oxidizing species in the cathode.

$$\text{Anode}: \ 2H_2O \rightarrow O_2\,(g) + 4H^+ + 4e^- \quad (13)$$

$$\text{Cathode}: \ 2H_2O + 2e^- \rightarrow H_2\,(g) + 2OH^- \quad (14)$$

$$O_2(g) + 2e^- + 2H^+ \rightarrow H_2O_2 \quad (15)$$

$$O_2\,(g) + H_2O + 2e^- \rightarrow OH^- + HO_2^- \quad (16)$$

$$H_2O_2 + HO_2^- \rightarrow OH^{\cdot} + O_2^{\cdot -} + H_2O \quad (17)$$

The average voltages reached during the regeneration at 70 A, are 6.7, 6.4, and 6.1 V for PPR1, PPR2, and PPR3, respectively. In the case of PPR1 the oxygen evolution reaction (OER) occurs at higher potentials in the anode, thus lower concentration of oxidizing species is formed, and more time is required for reaching the electrochemical regeneration. However, in the case of PPR2 and PPR3, the OER is produced at lower potentials and the time required to reach the maximum regeneration at current used is lower (Table 1).

Moreover, the electrocatalytic activity to OER has an influence in the surface chemistry of the regenerated ACs. Then, the most electrocatalytic anode for OER (PPR3) produces the higher oxidation of the AC (see Figs. 3, S**2** and Table 1). The decrease in S_{BET} values once the maximum value has been reached can be due to readsorption of desorbed compounds.

Thus, there are no significant differences between the anode material used during the regeneration process. Therefore, DSA can be used as an economical alternative due to their lower cost and minor voltage respect to the more expensive and lower electroactive Pt/Ti anode for the electrochemical regeneration of AC.

3.3. Concentric cylindrical reactor configuration

Fig. S**1** shows the N_2 adsorption-desorption isotherms for the pristine, spent and washed AC, and electrochemically regenerated ACs using the CCR configuration under the same electrochemical regeneration conditions. Table 2 summarizes the main textural properties. The results show that this reactor configuration permits a recovery of the porous texture using the three anodes studied, with a %RP above 90 % for the three anodes tested (Table 2). PSD included in Fig. S**1**, show that the regeneration produces a recovery of the porosity. The main difference with respect to the PPR configuration is that the time necessary to achieve the maximum recovery of porosity is higher for the CCR configuration.

TPD profiles obtained for the regenerated samples are presented in Fig. 3**B** (see Fig. S**2** for TPD profiles for RuO_2/Ti and IrO_2/Ti in the CCR configuration). Table 2 contains the amount of CO and CO_2 desorbed as well as the total oxygen content. As observed in the PPR configuration, the regeneration produces some increase in the surface oxidation of the AC compared to the spent AC after washing with the electrolyte. However, this increase in the amount of surface oxygen groups is smaller than in the PPR configuration. Narbaitz and Karimi-Jashni (2012) suggested that this may be since there is a greater fraction of AC particles in direct contact with the cathode since the surface of electrodes in PPR is greater than in CCR.

Both the increase in the regeneration time necessary for the recovery of the porosity and the lower degree of surface oxidation, agree with the lower specific charge used in this setup. In the CCR configuration the average voltage during the regeneration experiments, using with the same current density as with the PPR configuration, is lower (for CCR1, CCR2 and CCR3 reactors the average treatment voltage was 4.7, 4.2 and 4.2 V, respectively, whereas these values are 6.7, 6.4, and 6.1 V for PPR1, PPR2 and PPR3 reactors). The lower voltage achieved with this configuration results in a lower electric field and smaller concentration of oxidizing species, thus making the regeneration process slower.

3.4. Comparison of reactor configuration at pilot-plant scale

A comparison between the two proposed and designed reactors in terms of EC and regeneration cost is presented in Table 3. From these data, it can be seen that PPR configuration has several advantages over CCR configuration: i) the higher voltage results in a faster regeneration of the AC; ii) electricity consumption is lower and iii) the cost of the process is lower, using as the price of electricity in Spain 0.1527 €/kWh. However, PPR configuration has three disadvantages over the CCR configuration: i) greater oxidation of the materials; ii) the voltage of the process is higher, increasing the emission of gases resulting from the elec-

Table 2
Physicochemical characterization of textural properties by N_2 and CO_2 adsorption-desorption isotherms, TPD and pH_{PZC} of pristine, spent, washing and electrochemical regenerated AC in concentric cylindrical reactor configuration. All experiments were carried out with 10 kg of spent AC, under cathodic conditions, applying 27.5 A during 4 h, using 0.5 M H_2SO_4 as electrolyte solution and a flow rate of 750 L/h.

Sample	S_{BET} m^2/g	V_{DR},N_2 cm^3/g	V_{DR},CO_2 cm^3/g	V_{meso} cm^3/g	%RP	%AR	CO μmol/g	CO_2 μmol/g	O μmol/g	pH_{PZC}
Pristine	995	0.36	0.30	0.04			566	178	922	10.4
Spent	790	0.32	0.24	0.03			2668	1462	5592	7.3
Washing	870	0.35	0.25	0.04	87	39	2275	1361	4997	2.1
CCR1 (Pt/Ti)										
Reg-1h	855	0.35	0.29	0.03	86	32	2421	1001	4424	2.0
Reg-2h	815	0.33	0.26	0.04	82	12	2336	864	4064	1.8
Reg-3 h	950	0.38	0.27	0.04	96	78	2766	1068	4902	1.9
Reg-4h	830	0.34	0.26	0.03	83	20	3069	925	4919	1.9
CCR2 (RuO_2/Ti)										
Reg-1h	810	0.33	0.24	0.04	81	10	3252	1122	5496	2.2
Reg-2h	840	0.34	0.27	0.04	84	24	2773	997	4766	2.0
Reg-3 h	820	0.33	0.26	0.04	82	15	2138	878	3895	2.0
Reg-4h	900	0.36	0.27	0.04	91	54	2814	1069	4952	2.0
CCR3 (IrO_2/Ti)										
Reg-1h	895	0.36	0.27	0.04	90	51	2595	986	4566	2.4
Reg-2h	880	0.35	0.27	0.04	88	44	2737	971	4680	2.4
Reg-3 h	875	0.35	0.27	0.04	88	42	2742	966	4675	2.2
Reg-4h	935	0.37	0.27	0.04	94	71	2638	1025	4688	2.2

Table 3
Comparison of the two reactors at the pilot-plant scale designed for the electrochemical regeneration of AC used in DWTP.

Characteristics	PPR	CCR
AC capacity (kg)	15	10
Regeneration time (h)	1	4
Current (A)	70	27
Voltage (V)	6.7	4.8
Anode	RuO_2/Ti	IrO_2/Ti
Electrode area (cm^2)	2800	1080
%Recovery of porosity	95	94
%Adsorption recovery	76	71
Energy consumption (kWh/kg AC)	0.031	0.045
Electric cost (€/kg AC)	0.0047	0.0069

trolysis process; iii) the cost in electrodes is greater because of the higher geometric area. Regarding the residence time, due to its small difference, 168 s for PPR and 153 s for CCR, respectively, no effect should be expected in the final porosity of the regenerated ACs.

Regarding the effect of the configuration on the regeneration efficiency of ACs used in DWTP, if the experimental conditions are adequately selected for each reactor, the performance is similar.

Nevertheless, it should be noted that both reactors are capable of recovering the porous texture of spent AC in real conditions and that the two prototypes present a breakthrough in the electrochemical regeneration of carbon materials because both reactors have a much lower EC than those presented in different research at smaller scales, which are between 0.13–3.80 kW h/kg AC (Zhou and Lei, 2006; Weng and Hsu, 2008; Acuña-Bedoya et al., 2020). Regarding the production of new AC compared to the electrochemical regeneration, the reduction in cost goes from 1.84 kW h/kg AC (Bayer et al., 2005) to 0.031 and 0.045 kW h/kg AC for PPR and CCR configuration, respectively. In addition, there is a reduction in EC compared to our first prototype developed with a capacity for 3.5 kg of AC, that it was 0.11 kW h/kg (Ferrández-Gómez et al., 2021), demonstrating the efficiency of the scaling-up process. And if we compare electrochemical with industrial thermal regeneration (Muñoz et al., 2007), the EC decreases by more than 90 % for both reactors design. This work demonstrates the viability of the electrochemical method for the regeneration of AC at industrial level.

Regarding the SEM study, Fig. 4 shows the regenerated samples for PPR and CCR configuration using the Pt/Ti anode after 3 h of treatment. It can be observed that the treatment has removed the observable inorganic matter of the AC surface with respect to the spent AC sample. Table S**4** confirms that electrochemical treatment was able to partially eliminate the inorganic matter present in the spent AC sample. However, as previously studied, the total elimination of inorganic compounds is very difficult in ACs (Weng and Hsu, 2008).

3.5. Adsorption kinetics of bisphenol A and modelling

Although the porous texture of the spent AC can be recovered by the electrochemical regeneration, the surface chemistry is modified. The modification consists in surface oxidation that occurs mainly during its use in the DWTP. Thus, it is interesting to assess the performance of regenerated AC in the adsorption in solution of a model compound. In this case, we have tested the adsorption of BPA.

Fig. 5 shows the results of the kinetics of adsorption of BPA in pristine and regenerated ACs in both electrochemical reactors using the three anodes studied. Compared to the pristine AC, the adsorption capacity is not very different but the kinetics of adsorption for the electrochemically regenerated AC is slower. Since the porous texture of the ACs is similar, the slower kinetics can be due to the surface oxygen groups (Arampatzidou and Deliyanni, 2016).

The size of the BPA molecule is 0.383 nm x 0.587 nm x 1.068 nm, making that the adsorption mainly occurs in the micropores and mesopores of the material (Arampatzidou and Deliyanni, 2016; López-Ramón et al., 2019). Since the micropore volumes for the pristine and regenerated ACs selected are similar (see data for samples obtained in 1st and 4th h of treatment, respectively, for PPR and CCR configuration in Tables 1 and 2). This difference in adsorption kinetics must be related to the higher number of oxygen surface groups present in the electrochemically regenerated AC, that produce an impediment to the diffusion of the BPA into the micropores. This aspect was already discussed previously by other authors who observed that the degree of oxidation of the carbon material negatively affected the kinetics of adsorption of BPA (López-Ramón et al., 2019).

It is important to highlight that the mechanism of adsorption of BPA in ACs is due to the π-π interactions of the π electrons of the benzene rings of BPA with the π electrons of the ACs and

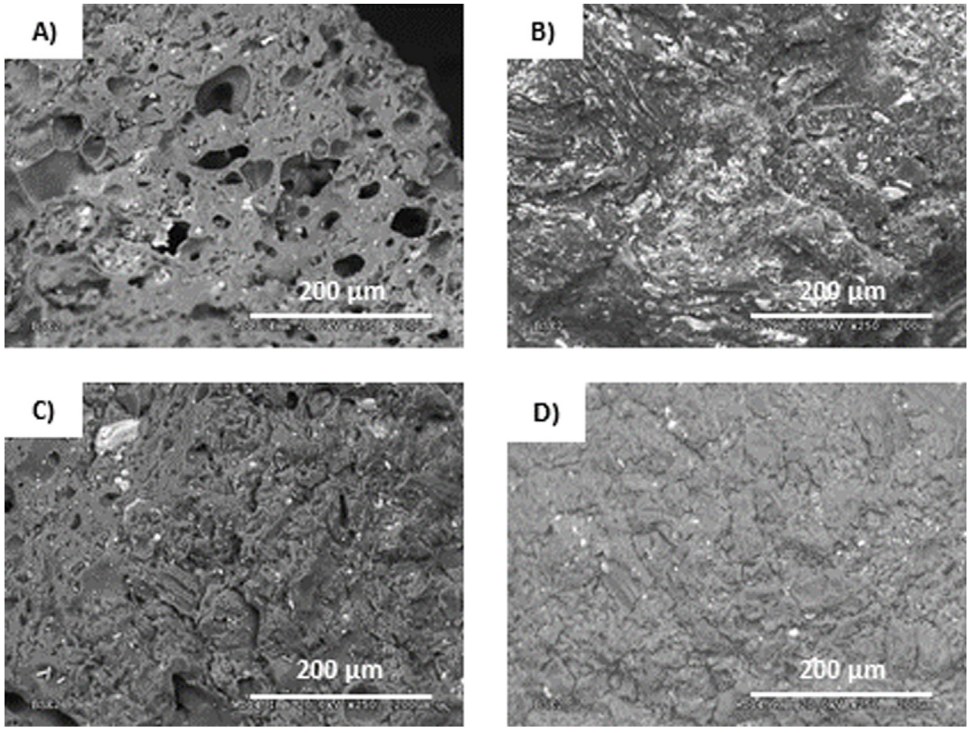

Fig. 4. SEM images (×250) of activated carbon surface: A) pristine, B) spent, C) PPR1-3 h (Pt/Ti) and D) CCR1-3 h (Pt/Ti).

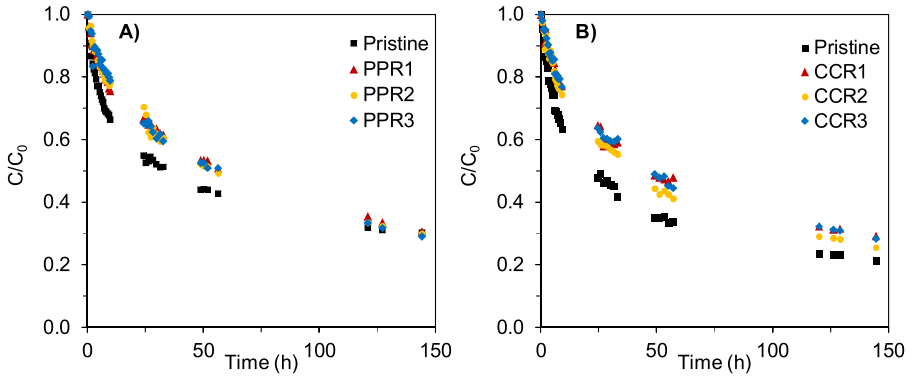

Fig. 5. BPA adsorption experiments at 25 °C and C_0 = 250 mg/L: A) AC samples regenerated after 1 h treatment in PPR configuration and B) AC samples regenerated after 4 h treatment in CCR configuration.

the hydrogen bond between the $^{-}$OH groups of BPA and the acidic oxygen-containing groups on the surface of the AC (Liu et al., 2009; Arampatzidou and Deliyanni, 2016). For this reason, the acidity or basicity of the AC surface plays an important role in the adsorption process.

To analyse the kinetics of adsorption we have applied the four models described in the experimental section. Fig. 6 and Fig. S**14** include the amount of BPA adsorbed *versus* time for the pristine AC and three ACs regenerated with the PPR and the CCR configuration, respectively. The parameters obtained from each kinetic model are summarized in Tables S**5–S6**.

In the case of the pristine AC, the results show that the models that better describe the adsorption of BPA are the pseudo-second order and Elovich models with a small difference in correlation coefficients. Both are models in which the adsorption process is controlled by the adsorption step.

However, the ACs regenerated with the PPR and CCR configuration show interesting differences with the pristine AC. In the case of PPR configuration, the kinetic data for the regenerated AC, fits better to the intraparticle diffusion model (Table S**5** and Fig. 6), although the best fit would be obtained with a mixture of pseudo-second order and intraparticle diffusion. The results are in agreement with the previous comments about the role of the surface oxygen groups in slowing down the BPA adsorption rate (Arampatzidou and Deliyanni, 2016; de Franco et al., 2017). In the case of CCR configuration, the pseudo-second order model produces higher correlation coefficients (Table S**6** and Fig. S**14**), what can be understood considering that, in general, this reactor produces a lower degree of surface oxidation at the experimental conditions used for the electrochemical regeneration. Then, the results clearly show the relevance of the surface oxygen groups on the kinetics of BPA adsorption. However, the adsorption capacities in all cases are similar to the pristine AC provided that the micropore volumes are close. Nevertheless, when comparing samples regenerated in PPR and CCR, the PBA adsorption capacity is somewhat higher for PPR in agreement with the slightly higher values of micropore volumes and %AR achieved with the PPR regeneration (Tables 1 and 2).

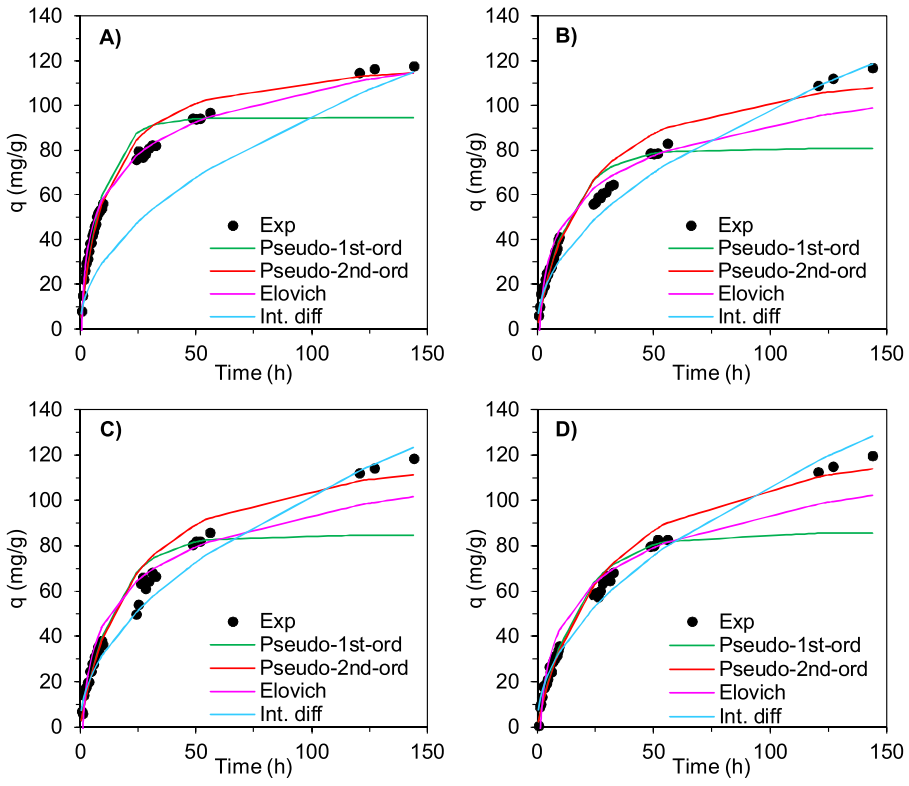

Fig. 6. Adsorption kinetics of BPA on the activated carbon samples regenerated in parallel plate electrochemical reactor configuration: A) pristine, B) PPR1, C) PPR2 and D) PPR3. The lines represent the prediction of a pseudo-first-order kinetic model, pseudo-second-order kinetic model, Elovich model and intraparticle diffusion model.

4. Conclusions

The electrochemical regeneration of spent activated carbon used in a water purification plant can be achieved using two different designs of pilot plant-scale reactors that work with 10–15 kg of AC. In both cases, at the adequate experimental conditions, a recovery of the porosity of around 95 % can be obtained. The results are promising for the scale-up to the future industrial application as an alternative to the traditional thermal regeneration.

The designed reactors achieved that regeneration efficiency with a drastic decrease in energy consumption compared to other electrochemical reactors used in AC regeneration. Both have their advantages and disadvantages, but it seems that greater contact between the electrode and the material to be regenerated produces a better recovery of the porous textural properties.

There are no significant differences between the anode material used during the regeneration process. A commercial DSA can be used as a cheaper and lower voltage anode as alternative to the more expensive commercial Pt/Ti in the electrochemical regeneration of AC. However, some additional oxidation of the carbon material with respect to the spent AC cannot be avoided what can be a negative feature of this method.

The adsorption of BPA by electrochemically regenerated ACs had slightly slower kinetics than the pristine AC due to the presence of oxygen groups on the surface of the material which are mainly formed during the use of the AC in the water treatment regeneration plant. However, the adsorption capacity at equilibrium conditions is similar provided that the compared materials have similar micropore volumes. Application of different kinetic models show that the presence of surface oxygen groups can produce a change in the rate determining step from the adsorption on a surface site to pore diffusion.

Finally, we can demonstrate the viability of the electrochemical method for the regeneration of AC at industrial level.

CRediT authorship contribution statement

Borja Ferrández-Gómez: Conceptualization, Methodology, Investigation, Writing - original draft. **Diego Cazorla-Amorós:** Conceptualization, Methodology, Supervision, Writing - review & editing, Funding acquisition. **Emilia Morallón:** Conceptualization, Methodology, Project administration, Supervision, Writing - review & editing, Funding acquisition.

Declaration of Competing Interest

The authors declare that they have no conflicts of interest.

Acknowledgement

This work was supported by the European Union-Horizon 2020 (PORTABLECRAC - SPIRE09 - 2017 Nº 768905).

Appendix A. Supplementary data

Supplementary material related to this article can be found, in the online version, at doi:https://doi.org/10.1016/j.psep.2021.02.007.

References

Acuña-Bedoya, J., Comas-Cabrales, J.A., Alvarez-Pugliese, C.E., Marriaga-Cabrales, N., 2020. Evaluation of electrolytic reactor configuration for the regeneration of granular activated carbon saturated with methylene blue. J. Environ. Chem. Eng. 8, 104074, http://dx.doi.org/10.1016/j.jece.2020.104074.

Ania, C.O., Béguin, F., 2008. Electrochemical regeneration of activated carbon cloth exhausted with bentazone. Environ. Sci. Technol. 42, 4500–4506, http://dx.doi.org/10.1021/es703192x.

Arampatzidou, A.C., Deliyanni, E.A., 2016. Comparison of activation media and pyrolysis temperature for activated carbons development by pyrolysis of potato peels

for effective adsorption of endocrine disruptor bisphenol-A. J. Colloid Interface Sci. 466, 101–112, http://dx.doi.org/10.1016/j.jcis.2015.12.003.
Bayer, P., Heuer, E., Karl, U., Finkel, M., 2005. Economical and ecological comparison of granular activated carbon (GAC) adsorber refill strategies. Water Res. 39, 1719–1728, http://dx.doi.org/10.1016/j.watres.2005.02.005.
Berenguer, R., Marco-Lozar, J.P., Quijada, C., Cazorla-Amorós, D., Morallón, E., 2009. Effect of electrochemical treatments on the surface chemistry of activated carbon. Carbon 47, 1018–1027, http://dx.doi.org/10.1016/j.carbon.2008.12.022.
Berenguer, R., Marco-Lozar, J.P., Quijada, C., Cazorla-Amorós, D., Morallón, E., 2010a. Electrochemical regeneration and porosity recovery of phenol-saturated granular activated carbon in an alkaline medium. Carbon 48, 2734–2745, http://dx.doi.org/10.1016/j.carbon.2010.03.071.
Berenguer, R., Marco-Lozar, J.P., Quijada, C., Cazorla-Amorós, D., Morallón, E., 2010b. Comparison among chemical, thermal, and electrochemical regeneration of pheno-saturated activated carbon. Energy Fuels 24, 3366–3372, http://dx.doi.org/10.1021/ef901510c.
Brown, N.W., Roberts, E.P.L., Chasiotis, A., Cherdron, T., Sanghrajka, N., 2004. Atrazine removal using adsorption and electrochemical regeneration. Water Res. 38, 3067–3074, http://dx.doi.org/10.1016/j.watres.2004.04.043.
Dai, Y.D., Yuan, C., Huang, C.P., Chiang, P.C., 2017. Regeneration of spent carbon nanotubes by electrochemical oxidation over RuO_2/Ti electrode. Sep. Purif. Technol. 178, 207–214, http://dx.doi.org/10.1016/j.seppur.2017.01.021.
de Franco, M.A.E., de Carvalho, C.B., Bonetto, M.M., Soares, R., de, P., Féris, L.A., 2017. Removal of amoxicillin from water by adsorption onto activated carbon in batch process and fixed bed column: kinetics, isotherms, experimental design and breakthrough curves modelling. J. Clean. Prod. 161, 947–956, http://dx.doi.org/10.1016/j.jclepro.2017.05.197.
Delpeux-Ouldriane, S., Gineys, M., Cohaut, N., Béguin, F., 2015. The role played by local pH and pore size distribution in the electrochemical regeneration of carbon fabrics loaded with bentazon. Carbon 94, 816–825, http://dx.doi.org/10.1016/j.carbon.2015.07.010.
Ding, H., Zhu, Y., Wu, Y., Zhang, J., Deng, H., Zheng, H., Liu, Z., Zhao, C., 2020. *In Situ* regeneration of phenol-saturated activated carbon fiber by an electro-peroxymonosulfate process. Environ. Sci. Technol., http://dx.doi.org/10.1021/acs.est.0c03766.
Dubinin, M.M., 1960. The potential theory of adsorption of gases and vapors for adsorbents with energetically nonuniform surfaces. Chem. Rev. 60, 235–241, http://dx.doi.org/10.1021/cr60204a006.
Ferrández-Gómez, B., Ruiz-Rosas, R., Beaumont, S., Cazorla-Amorós, D., Morallón, E., 2021. Electrochemical regeneration of spent activated carbon from drinking water treatment plant at different scale reactors. Chemosphere 264, 128399, http://dx.doi.org/10.1016/j.chemosphere.2020.128399.
Figueiredo, J., Pereira, M.F., Freitas, M.M., Órfão, J.J., 1999. Modification of the surface chemistry of activated carbons. Carbon 37, 1379–1389, http://dx.doi.org/10.1016/S0008-6223(98)00333-9.
Gineys, M., Benoit, R., Cohaut, N., Béguin, F., Delpeux-Ouldriane, S., 2017. Behavior of activated carbon cloths used as electrode in electrochemical processes. Chem. Eng. J. 310, 1–12, http://dx.doi.org/10.1016/j.cej.2016.10.018.
Grupioni, A.A.F., Arashiro, E., Lassali, T.A.F., 2002. Voltammetric characterization of an iridium oxide-based system: the pseudocapacitive nature of the $Ir_{0.3}Mn_{0.7}O_2$ electrode. Electrochim. Acta 48, 407–418, http://dx.doi.org/10.1016/S0013-4686(02)00686-2.
Ho, Y., McKay, G., 1999. Pseudo-second order model for sorption processes. Process Biochem. 34, 451–465, http://dx.doi.org/10.1016/S0032-9592(98)00112-5.
Huang, X., An, D., Song, J., Gao, W., Shen, Y., 2017. Persulfate/electrochemical/$FeCl_2$ system for the degradation of phenol adsorbed on granular activated carbon and adsorbent regeneration. J. Clean. Prod. 165, 637–644, http://dx.doi.org/10.1016/j.jclepro.2017.07.171.
Jagiello, J., Olivier, J.P., 2012. 2D-NLDFT adsorption models for carbon slit-shaped pores with surface energetical heterogeneity and geometrical corrugation. Carbon 55, 70–80, http://dx.doi.org/10.1016/j.carbon.2012.12.011.
Kamgaing, T., Doungmo, G., Melataguia Tchieno, F.M., Gouoko Kouonang, J.J., Mbadcam, K.J., 2017. Kinetic and isotherm studies of bisphenol A adsorption onto orange albedo (*Citrus sinensis*): sorption mechanisms based on the main albedo components vitamin C, flavones glycosides and carotenoids. J. Environ. Sci. Heal. 52, 757–769, http://dx.doi.org/10.1080/10934529.2017.1303315.
Karabacakoğlu, B., Savlak, Ö., 2014. Electrochemical regeneration of Cr(VI) saturated granular and powder activated carbon: comparison of regeneration efficiency. Ind. Eng. Chem. Res. 53, 13171–13179, http://dx.doi.org/10.1021/ie500161d.
Krstić, V., Pešovski, B., 2019. Reviews the research on some dimensionally stable anodes (DSA) based on titanium. Hydrometallurgy 185, 71–75, http://dx.doi.org/10.1016/j.hydromet.2019.01.018.
Lagergren, S., 1898. Zurtheorie der sogenannten adsorption gelosterstoffe, Kungliga Svenska Vetenskapsakademiens. Handlingar 24, 1–39.
Liu, G., Ma, J., Li, X., Qin, Q., 2009. Adsorption of bisphenol A from aqueous solution onto activated carbons with different modification treatments. J. Hazard. Mater. 164, 1275–1280, http://dx.doi.org/10.1016/j.jhazmat.2008.09.038.
Liu, S., Wang, Y., Wang, B., Huang, J., Deng, S., Yu, G., 2017. Regeneration of rhodamine B saturated activated carbon by an electro-peroxone process. J. Clean. Prod. 168, 584–594, http://dx.doi.org/10.1016/j.jclepro.2017.09.004.
Liu, Z., Ren, B., Ding, H., He, H., Deng, H., Zhao, C., Wang, P., Dionysiou, D.D., 2020. Simultaneous regeneration of cathodic activated carbon fiber and mineralization of desorbed contaminations by electro-peroxydisulfate process: advantages and limitations. Water Res. 171, 115456, http://dx.doi.org/10.1016/j.watres.2019.115456.
López-Ramón, M.V., Ocampo-Pérez, R., Bautista-Toledo, M.I., Rivera-Utrilla, J., Moreno-Castilla, C., Sánchez-Polo, M., 2019. Removal of bisphenols A and S by adsorption on activated carbon clothes enhanced by the presence of bacteria. Sci. Total Environ. 669, 767–776, http://dx.doi.org/10.1016/j.scitotenv.2019.03.125.
Lozano-Castelló, D., Suárez-García, F., Cazorla-Amorxós, D., Linares-Solano, A., 2009. Porous texture of carbons. In: Beguin, F., Frackowiak, E. (Eds.), Carbons for Electrochemical Energy Storage and Conversion Systems. CRC Press, pp. 115–163.
Martínez-Huitle, C.A., Rodrigo, M.A., Sirés, I., Scialdone, O., 2015. Single and coupled electrochemical processes and reactors for the abatement of organic water pollutants: a critical review. Chem. Rev. 115, 13362–13407, http://dx.doi.org/10.1021/acs.chemrev.5b00361.
McQuillan, R.V., Stevens, G.W., Mumford, K.A., 2018. The electrochemical regeneration of granular activated carbons: a review. J. Hazard. Mater. 355, 34–49, http://dx.doi.org/10.1016/j.jhazmat.2018.04.079.
Moore, B.C., Cannon, F.S., Metz, D.H., DeMarco, J., 2003. GAC pore structure in Cincinnati during full-scale treatment/reactivation. J./Am. Water Work. Assoc. 95, 103–112, http://dx.doi.org/10.1002/j.1551-8833.2003.tb10296.x.
Muñoz, I., Peral, J., Antonio Ayllón, J., Malato, S., José Martin, M., Yves Perrot, J., Vincent, M., Domènech, X., 2007. Life-cycle assessment of a coupled advanced oxidation-biological process for wastewater treatment: comparison with granular activated carbon adsorption. Environ. Eng. Sci. 24, 638–651, http://dx.doi.org/10.1089/ees.2006.0134.
Narbaitz, R.M., Karimi-Jashni, A., 2012. Electrochemical reactivation of granular activated carbon: impact of reactor configuration. Chem. Eng. J. 197, 414–423, http://dx.doi.org/10.1016/j.cej.2012.05.049.
Narbaitz, R.M., McEwen, J., 2012. Electrochemical regeneration of field spent GAC from two water treatment plants. Water Res. 46, 4852–4860, http://dx.doi.org/10.1016/j.watres.2012.05.046.
Pletcher, D., Walsh, F.C., 1993. Industrial Electrochemistry. Springer Netherlands. Springer Netherlands, Dordrecht, http://dx.doi.org/10.1007/978-94-011-2154-5.
Radovic, R.L., Moreno-Castilla, C., Rivera-Utrilla, J., 2001. Carbon materials as adsorbents in aqueous solutions. In: Radovic, L.R. (Ed.), Chemistry and Physics on Carbon. Dekker, New York, pp. 227–405.
Rivera-Utrilla, J., Sánchez-Polo, M., Gómez-Serrano, V., Álvarez, P.M., Alvim-Ferraz, M.C.M., Dias, J.M., 2011. Activated carbon modifications to enhance its water treatment applications. An overview. J. Hazard. Mater. 187, 1–23, http://dx.doi.org/10.1016/j.jhazmat.2011.01.033.
Salvador, F., Martin-Sanchez, N., Sanchez-Hernandez, R., Sanchez-Montero, M.J., Izquierdo, C., 2015a. Regeneration of carbonaceous adsorbents. Part I: thermal regeneration. Microporous Mesoporous Mater. 202, 259–276, http://dx.doi.org/10.1016/j.micromeso.2014.02.045.
Salvador, F., Martin-Sanchez, N., Sanchez-Hernandez, R., Sanchez-Montero, M.J., Izquierdo, C., 2015b. Regeneration of carbonaceous adsorbents. Part II: chemical, microbiological and vacuum regeneration. Microporous Mesoporous Mater. 202, 277–296, http://dx.doi.org/10.1016/j.micromeso.2014.08.019.
Santos, D.H.S., Duarte, J.L.S., Tonholo, J., Meili, L., Zanta, C.L.P.S., 2020. Saturated activated carbon regeneration by UV-light, H_2O_2 and Fenton reaction. Sep. Purif. Technol. 250, 117112, http://dx.doi.org/10.1016/j.seppur.2020.117112.
Shabir, F., Sultan, M., Miyazaki, T., Saha, B.B., Askalany, A., Ali, I., Zhou, Y., Ahmad, R., Shamshiri, R.R., 2020. Recent updates on the adsorption capacities of adsorbent-adsorbate pairs for heat transformation applications. Renewable Sustainable Energy Rev. 119, 109630, http://dx.doi.org/10.1016/j.rser.2019.109630.
Sharif, F., Gagnon, L.R., Mulmi, S., Roberts, E.P.L., 2017. Electrochemical regeneration of a reduced graphene oxide/magnetite composite adsorbent loaded with methylene blue. Water Res. 114, 237–245, http://dx.doi.org/10.1016/j.watres.2017.02.042.
Such-Basáñez, I., Román-Marıínez, M.C., Salinas-Marıínez de Lecea, C., 2004. Ligand adsorption on different activated carbon materials for catalyst anchorage. Carbon 42, 1357–1361, http://dx.doi.org/10.1016/j.carbon.2004.01.015.
Thommes, M., Kaneko, K., Neimark, A.V., Olivier, J.P., Rodriguez-Reinoso, F., Rouquerol, J., Sing, K.S.W., 2015. Physisorption of gases, with special reference to the evaluation of surface area and pore size distribution (IUPAC Technical Report). Pure Appl. Chem. 87, 1051–1069, http://dx.doi.org/10.1515/pac-2014-1117.
Ureta-Zañartu, M.S., Yáñez, C., Páez, M., Reyes, G., 1996. Electrocatalytic oxidation of ethylene glycol in 0.5 M H_2SO_4 and 0.5 M NaOH solutions at a bimetallic deposited electrode. J. Electroanal. Chem. 405, 159–167, http://dx.doi.org/10.1016/0022-0728(95)04407-8.
Walsh, F.C., Ponce de León, C., 2018. Progress in electrochemical flow reactors for laboratory and pilot scale processing. Electrochim. Acta 280, 121–148, http://dx.doi.org/10.1016/j.electacta.2018.05.027.
Wang, L., Balasubramanian, N., 2009. Electrochemical regeneration of granular activated carbon saturated with organic compounds. Chem. Eng. J. 155, 763–768, http://dx.doi.org/10.1016/j.cej.2009.09.020.
Weber, W.J., Morris, J.C., 1963. Kinetics of adsorption carbon from solutions. J. Sanit. Engeering Div. Proc. Am. Soc. Civ. Eng. 89, 31–60.
Weng, C.H., Hsu, M.C., 2008. Regeneration of granular activated carbon by an electrochemical process. Sep. Purif. Technol. 64, 227–236, http://dx.doi.org/10.1016/j.seppur.2008.10.006.
Xiao, C., Wang, L., Zhou, Q., Huang, X., 2020. Hazards of bisphenol A (BPA) exposure: a systematic review of plant toxicology studies. J. Hazard. Mater. 384, 121488, http://dx.doi.org/10.1016/j.jhazmat.2019.121488.
Zanella, O., Tessaro, I.C., Féris, L.A., 2014. Desorption- and decomposition-based techniques for the regeneration of activated carbon. Chem. Eng. Technol. 37, 1447–1459, http://dx.doi.org/10.1002/ceat.201300808.

Zanella, O., Bilibio, D., Priamo, W.L., Tessaro, I.C., Féris, L.A., 2017. Electrochemical regeneration of phenol-saturated activated carbon–proposal of a reactor. Environ. Technol. 38, 549–557, http://dx.doi.org/10.1080/09593330.2016.1202327.

Zhan, J., Wang, Y., Wang, H., Shen, W., Pan, X., Wang, J., Yu, G., 2016. Electro-peroxone regeneration of phenol-saturated activated carbon fiber: the effects of irreversible adsorption and operational parameters. Carbon 109, 321–330, http://dx.doi.org/10.1016/j.carbon.2016.08.034.

Zhan, J., Li, Z., Yu, G., Pan, X., Wang, J., Zhu, W., Han, X., Wang, Y., 2018. Enhanced treatment of pharmaceutical wastewater by combining three-dimensional electrochemical process with ozonation to *in situ* regenerate granular activated carbon particle electrodes. Sep. Purif. Technol., 0–1, http://dx.doi.org/10.1016/j.seppur.2018.06.030.

Zhou, M.H., Lei, L.C., 2006. Electrochemical regeneration of activated carbon loaded with p-nitrophenol in a fluidized electrochemical reactor. Electrochim. Acta 51, 4489–4496, http://dx.doi.org/10.1016/j.electacta.2005.12.028.